Royal Netherlands Institute for Sea Research

This is a pre-copyedited, author-produced version of an article accepted for publication, following peer review.

[Article begins on next page]

1   Indicators of expansion and retreat of *Phragmites* based on optical and radar satellite remote

2   sensing: a case study on the Danube delta

3

4   **Authors:**

5   Bas Oteman[1], Albert Scrieciu[2], Tjeerd Joris Bouma[1], Adrian Stanica[2], Daphne van der Wal[1,3]

6

7   [1]   NIOZ Royal Netherlands Institute for Sea Research, Department of Estuarine and Delta Systems, P.O. Box 140, 4400

8   AC Yerseke, the Netherlands.

9   [2]   GeoEcoMar Romanian National Institute for Research and Development for Marine Geology and Geo-ecology, Str.

10   Dimitrie Onciul 23-25, sector 2, 024053, Bucharest, Romania

11   [3]   Faculty of Geo-Information Science and Earth Observation (ITC), University of Twente, P.O. Box 217, 7500 AE

12   Enschede, The Netherlands.

13   *correspondence: basoteman@gmail.com, TEL: +31 (0)113 577 300

14

15   **Abstract**

16   Reed is an important wetland species. In some places it provides valuable ecosystem services, while in

17   other places it poses a threat as an invasive species. Thus, monitoring and predicting reed dynamics is

18   crucial. We not only detected changes in reed area using remote sensing, but also developed indicators

19   for the stability of reed wetlands based on remote sensing that would allow to predict its future

20   development. We used satellite imagery to study reed development in the Danube Delta in Romania over

21   a period of 22-years and identified expanding, stable and retreating reedlands. We then compared optical

22   vegetation indices and radar backscatter among those three different reed development categories. We

23   found clear spatial differences in long-term reed dynamics. We also revealed a clear difference in radar

24   backscatter, but no difference in the optical signal of expanding, stable and decreasing reed areas. The

25 radar data showed the largest seasonal variation in locations where reed was expanding and smallest

26 seasonal variation where reed was decreasing.

27 Overall, our study shows that the stability of reed ecosystems, and their services, can be monitored by

28 quantifying seasonal changes in backscatter of reed-lands using radar satellites. This principle looks

29 promising for monitoring other ecosystems as well.

30

31 **Keywords**

32 Reed, reed development, marsh, wetland, remote sensing, radar, Danube delta

33

34 **1. Introduction**

35 Wetland ecosystems provide valuable services. For example, they provide habitats for unique plant

36 species and animal communities which may in part serve as food (Henderson and Lewis 2008, de Groot

37 et al. 2011). They also provide economic benefits (Henderson and Lewis 2008, Chmura 2011) and a nursery

38 for fish, thereby supporting local fisheries (Boesch and Turner 1984, Deegan et al. 2002, Chmura 2011). In

39 addition, wetlands may reduce nutrient loading in the coastal waters (Chmura 2011) and serve to mitigate

40 waves and reduce flood risk (Möller 2006, Barbier et al. 2008, Koch et al. 2009, Morgan et al. 2009, Chmura

41 2011, de Groot et al. 2011). Monitoring the stability and edge dynamics of wetlands, and thereby the

42 ecosystem services they provide, is thus important to enable suitable management.

43

44 Here, we focus on the stability of reed wetlands. Reed (*Phragmites australis*) is a common plant in

45 wetlands and is well known for its phytoremediation (Guo et al. 2014), but is also recognized as an

46 important species for shoreline protection, and protection of arthropods, birds and mammals (Ostendorp

47 et al. 2003, Cerri et al. 2017). Reed also provides raw materials, and can provide food for livestock (Stanica

48 et al. 2012). The function of reed as a buffer between aquatic and terrestrial ecosystems makes reed one

49   of the most important wetland species (Brix 1999). Since the 1950's, reed has shown a severe die-back in

50   eastern, central and northern Europe. This phenomenon was named the Reed Die-Back Syndrome (RDBS).

51   The warmer Mediterranean region did not seem affected, and reed here even seemed to expand rapidly

52   (Van Der Putten 1997). However, more recently reed die-back was also detected in Italy (Fogli et al. 2002,

53   Cerri et al. 2017).

54

55   In contrast to the reed die-back in northern Europe, in the United States reed is rapidly expanding and

56   commonly treated as an unwanted invasive species. In the US reed eradication programs are a common

57   part of management (Chambers et al. 1999, Silliman and Bertness 2004). Recently it has been suggested

58   that the European subspecies of reed is outcompeting the North American subspecies, with large potential

59   effects for the ecosystem, as reed can have a large effect on the nitrogen balance of a system (Findlay et

60   al. 2002, Volesky et al. 2018). Rapid expansion of reed lands in North America could indicate replacement

61   by the European subspecies.

62

63   Many possible causes of reed die-back or reed expansion have been suggested (Van Der Putten 1997,

64   Fogli et al. 2002, Cerri et al. 2017), but as of yet it is unclear which set of conditions are linked with these

65   developments. Hence, we lack reliable methods to predict where die-back or expansion may occur.

66   Remote sensing is a promising technique for both monitoring long-term reed dynamics as well as

67   obtaining indicators for predicting future reed development.

68

69   In this study we aim to take the first steps towards developing remote sensing techniques to both monitor

70   and predict future reed development. We will do this for the Danube delta along the Black Sea coast in

71   South Eastern Europe, one of the worlds` largest area naturally covered by wetlands. Here, reeds have

72   been continuously harvested for centuries and local communities greatly depend upon their many

73 ecosystem services (Stanica et al. 2012). The Razelm Sinoe Lagoon System, in the Danube Delta in Romania

74 was chosen as the study area. This lagoon system at the end of the Danube river, along the Black Sea

75 provides a massive coastline covered almost exclusively by reed, which is very important for local

76 communities (Stanica et al. 2012). It is unclear if the Danube delta follows the southern European trend

77 of rapid expansion, or if there are signs of vegetation die-back like sites in Italy (Fogli et al. 2002, Cerri et

78 al. 2017) and Hungary (Van Der Putten 1997).

79

80 To effectively monitor the vast area of the Razelm Sinoe Lagoon System ($\pm 1000 km^2$), we use space borne

81 remote sensing. Several studies have already looked into detecting reed using remote sensing to support

82 management; reed and other vegetation can be distinguished using optical (Pengra et al. 2007) or radar

83 data (Bourgeau-Chavez et al. 2013). In the south of France, an extensive model was used to model reed

84 height, diameter, flower head density, stem density and cover based on six optical satellite (SPOT 5)

85 images covering a single growing season (Poulin et al. 2010). They found that although the Normalized

86 Difference Vegetation Index (NDVI) performed poorly, the Soil Adjusted Vegetation Index (SAVI) worked

87 well. Space borne X-band radar has been applied to differentiate between reed, *Suaeda japonica*, and

88 mudflat (Lee et al. 2012). C-band radar has been shown to be useful to classify wetlands into six different

89 classes (forested and nonforested peat bogs, marsh, open water, clearing and forests) (Baghdadi et al.

90 2001). Sentinel 1's C-band Synthetic Aperture Radar (SAR) is expected to be very useful for wetland

91 analyses (Reschke et al. 2012). A study (Brisco et al. 2011) using airborne C-band radar found that reed

92 produces backscatter patterns similar to other grasses. Following the Freeman-Durden model (Freeman

93 and Durden 1998), they distinguished between double bounce scattering, volume scattering and surface

94 scattering and considered *Phragmites* a volume scattering object (Brisco et al. 2011). In other words, they

95 expect most of the signal to be scattered by the vegetation layer. Both optical and radar remote sensing

96 have been applied with success to reed monitoring before (Poulin et al. 2010, Lee et al. 2012). Several

97   studies have thus demonstrated the (change) detection of reed using remote sensing data, but without

98   predicting how this situation will develop in future. In this study we ultimately aim to identify a remote

99   sensing based indicator of future development, i.e., to signal where changes could be expected.

100

101   In this study, we will use a large historical optical satellite data set (the Landsat archive) to establish reed

102   development over a period of 22 years, and distinguish between increasing (lateral expansion), decreasing

103   (lateral loss) and stable reed areas. We detect differences in the state of reed areas, by comparing the

104   signals of optical (Sentinel 2 Multi Spectral Instrument) and radar (Sentinel 1 C-band Synthetic Aperture

105   Radar) in the three categories of reed development. Additionally we investigate the effect of the fetch

106   (the length of the open area the wind and waves have to build), as it has been suggested to influence

107   expansion (Coops et al. 1994) and we establish the effect of seasonal development patterns, as we expect

108   that a stressed system might have a smaller lateral expansion of reed in spring. Seasonal in situ

109   measurements in the Razelm Sinoe Lagoon System were taken to establish the underlying physical

110   characteristics of the reed beds.

111

112   Summarizing, the overarching aim of this study is to establish an indicator to help monitor reed dynamics,

113   and hence the stability of the ecosystem services the reed provides. We do so by focusing on indicators

114   that can be derived from satellite remote sensing data, and that distinguish between areas with die-back

115   versus expansion. We subsequently apply this indicator to a major coastal reed land in the Razelm Sinoe

116   Lagoon System in Romania, to establish if reed wetlands are dying back or expanding. This will directly

117   support monitoring efforts in Romania, but might also be a first step towards mapping reed die-back or

118   expansion in other areas.

119

120

2. Materials and methods

In this section we first describe the study area followed by the protocol for the in situ measurements. We then establish where expansion, minor change and retraction of reed has taken place, by comparing two satellite images from the Landsat archive, 22 years apart. This is followed by an explanation on how we established reed development within these 22 years every 2-4 years. Subsequently, we describe how we calculated the fetch length. Finally, we describe how we use indices from recent optical (Sentinel 2 MSI) and radar (Sentinel 1 SAR) satellite images to compare expanding, stable and eroding reed areas in winter, spring and summer.

Area description

The primary study site is the Razelm Sinoe Lagoon System, in Romania. This is the southern part of the Danube Delta Biosphere Reserve. The entire system covers about 1000km^2, and consists of a series of lakes, former lagoons transformed into lakes and present-day lagoons with engineered inlets, as well as other ponds, wetlands, former coastal sandbars, fossil and present day littoral barrier beaches. The coastal vegetation consists mainly of reed (*Phragmites australis*) which can grow up to six meters, before dying in winter (Hanganu et al. 2002). The lagoon has seen major human influences over the last century. The connection with the nearby fresh water system, the Danube, was increased by cutting new canals and dredging existing channels, followed by closing down of the main inlet in 1974 (at Gura Portitei) and replacement of the natural connections with the sea with engineered inlets (for Sinoe Lagoon). This caused the system to move towards a fresh water system. This also meant an increase of Danube-born nutrient and sediment inflow in the lagoon system. The limited connection with the sea causes the system to accumulate both organic and non-organic matter (Stanica et al. 2012, Dinu et al. 2015). The climate of the Lagoon System is continental, with hot dry summers and very cold winters. The Lagoon System is located in one of the windiest areas in Romania. The water bodies of the lagoon system are partly or

145   entirely frozen during winter, the freezing periods vary from days to weeks, but complete ice cover for

146   long periods is rare.

147

148   **Seasonal in situ measurements of reed characteristics**

149   At two locations in the Razelm Sinoe Lagoon System, in situ measurements were taken, the first site,

150   Jurilovca (see figure 1), is located at latitude: 44.75°, longitude: 28.94°, the second site, Histria, is located

151   at latitude: 44.55°, longitude: 28.78°. Site Jurilovca was sampled in March, May and July 2015. Site Histria

152   was sampled in the same months in 2016 (see appendix 1 for a detailed map of both sites). Five destructive

153   plots and six non-destructive plots of 1x1m were placed at both sites. The position of each plot was

154   recorded with a GPS. In each plot, the number of reed stems was counted by placing a 0.5x0.5 m frame

155   and counting all stems with a length > 30 cm, stems with a shorter length were ignored. In each plot, 20

156   representative stems are selected, their diameter is measured approximately 10 centimeter above the

157   ground. These stems were harvested and their length was recorded. They were weighed, dried for >3 days

158   at 60° and reweighed to establish wet and dry biomass.

159

160

161

162 **Figure 1: the first field site, Jurilovca. Picture taken by D. van der Wal at the 29th of April 2015.**

163

164 **Categorizing long-term vegetation development from Landsat imagery (22 years)**

165 To establish vegetation development in the Razelm Sinoe Lagoon System we used two Landsat images 22

166 years and 4 days apart (Landsat 5 TM at 1995-07-04 and Landsat 8 OLI at 2017-06-30). We used the surface

167 reflectance images provided by the United States Geological Survey (USGS), made available through

168 EarthExplorer. The rough outlines of the lagoon were manually drawn, to ensure we only have vegetation

169 and water in the area of interest and all roads and other human structures are excluded. This outline was

170 made manually, and is of variable width. The aim of this outline is to exclude anything that is not reed or

171 water e.g., inland vegetation, roads etc), thus retaining only the wetland area. Within this rough area of

172 interest we established the land line by applying a threshold of 0.3 on the Normalized Difference

173 Vegetation Index (NDVI). This is done for both images (1995 and 2017). Both water lines were visually

174 checked and the NDVI threshold performed well. In the Razelm Sinoe Lagoon System, a small section at

175 the southern tip of Sinoe lake was removed from analyses, as it proved difficult to distinguish between

176 water and vegetation here in the 2017 image, likely due to a mix of dead vegetation, water and sediment.

177 This small section was not taken into consideration for any of the consecutive analyses. In addition, some

178 areas were excluded due to clouds and cloud shadows in the imagery. Appendix 2 provides the outline of

179 the applied masks.

180 This study is focused on reed retraction or expansion by looking at vegetation stress at the seaward edge

181 of the wetland vegetation. If we include the broader reed land, any signal of stress caused by edge effects

182 may not be detectable. Therefore we extract a small strip that can reasonably be expected to show this

183 stress. We used the water edge of 2017 to extract a strip of 60m (i.e. 2 Landsat pixels) of reed vegetation.

184 For pixels in this strip, the lateral development of the reeds (stable, increase or decrease) was established.

185 Within this strip, values were extracted every 30m, which is the spatial resolution of the Landsat imagery.

186 The distance to the water was calculated for each pixel in each image; this distance was used to distinguish

187 between increasing, stable and decreasing pixels. A pixel with an unchanged distance to water or a pixel

188 where this distance is larger than 45 meters in both 1995 and 2017 was classified as stable (see figure 2).

189 We use 45m because this is roughly the diagonal of one Landsat pixel (42.43m), so in this case there is at

190 least a full pixel in front of this vegetation pixel that can absorb any stress that originates from the water-

191 vegetation border.

192 The remaining pixels were divided as: decrease < 0 < increased. Note that the pixels that were in the area

193 with decreased reeds were still vegetated (as by definition pixels with vegetation in 2017 were selected).
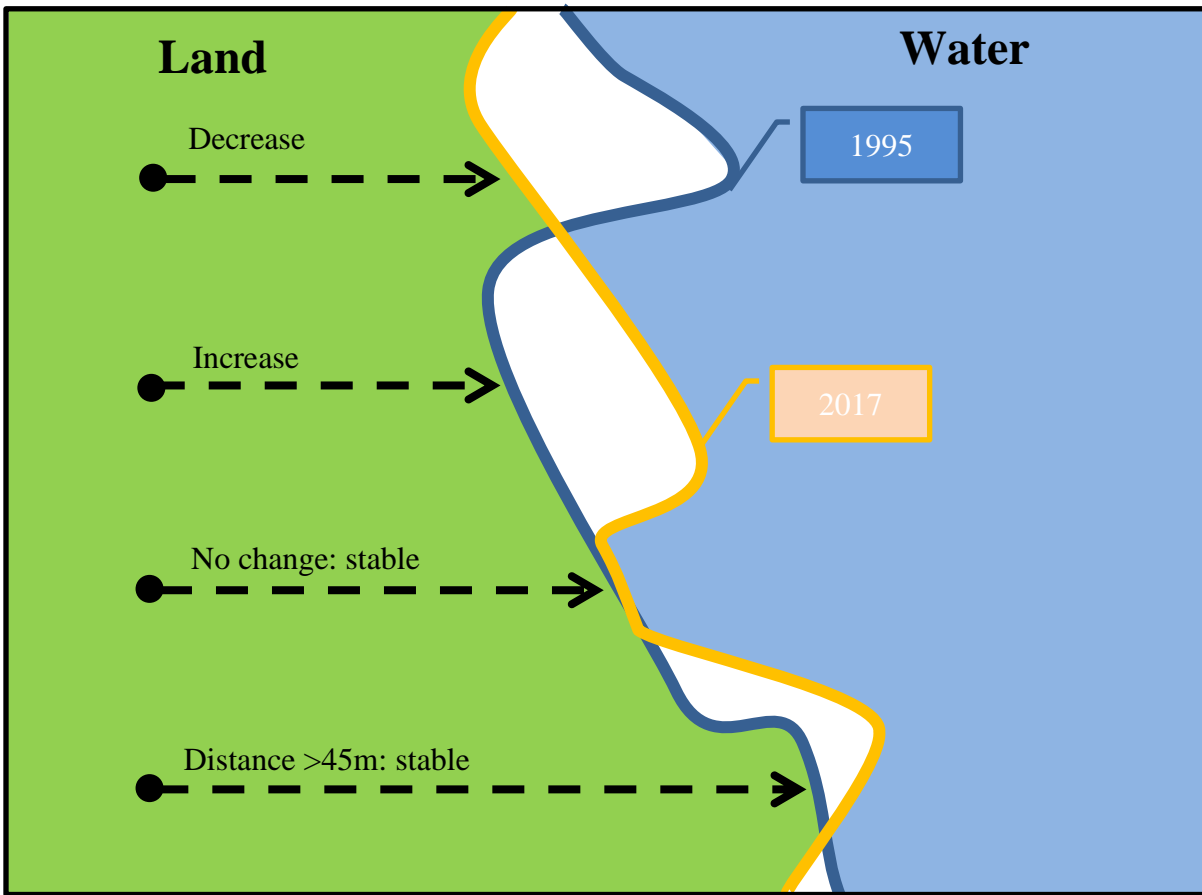
194

Figure 2: Schematization of assigning the reed development categories (decrease, stable, increase) based on shoreline changes between 1995 and 2017.

Establishing long-term reed development from Landsat imagery (2-4 year steps)

To gain further insight into the long-term reed development, we analyzed six additional Landsat images (of: 1999, 2001, 2005, 2008, 2011 and 2015, see table 1). We processed these similarly to the previous Landsat images and calculated the distance to the water for each sampling point. We tested the performance of our manual threshold of NDVI (as used to establish the development categories from the 1995 and 2017 images), by applying the ArcGIS tool 'Iso Cluster Unsupervised Classification' (using 2 classes) to the sequence of NDVI maps. This consistently estimated the land water threshold at an NDVI

219   between 0.25 and 0.3. We used the unsupervised clustering threshold analyses to distinguish between

220   land and water.

221   We used images from the same season (June/July) and used a compounding cloud mask (i.e. pixels that

222   were covered by clouds or cloud shadows in any year were completely removed from the analysis). For

223   the pixels in the selected strip along the shoreline, we then analyzed the position of the pixels relative to

224   the shoreline, for the three reed development categories (retreat, stable and expansion). We used the

225   development categories established between 1995-2017 to compare the distance to the water edge

226   between categories. This provided insight into the persistence of the reed development.

227

228   Table 1, Landsat images of the Razelm Sinoe Lagoon System for multi-year analysis.

Satellite	Date
Landsat 5	1999-06-29
Landsat 5	2001-07-04
Landsat 5	2005-06-29
Landsat 5	2008-07-07
Landsat 5	2011-07-16
Landsat 8	2015-07-11

229

230

231   **Establishing wave exposure of reeds, using fetch length from Landsat imagery**

232   Based on the established vegetation edge for the Landsat 8 image of 2017-06-30, the so-called fetch was

233   calculated, indicating the length over which wind-waves can build up over water. To establish the fetch,

234   we determined the angle towards the water using the direction raster of the Euclidean Distance tool in

235   ArcGIS. The fetch was then calculated as the distance in that direction until land (on the opposite side of

236   the lagoon) was reached. Given the jagged shoreline, land closer than 100m was not considered as the

237   opposite side of the lagoon, and was ignored. Note that in this study, fetch was calculated for the onshore

238   direction only (i.e., perpendicular to the coastline), and it is thus independent of actual wind direction.

239   For each of the reed development categories (increase, stable, decrease) the mean fetch length was

240   established to test whether shoreline change depended on the exposure of the reed to wind-waves.

241

242   **Analyzing seasonal remote sensing indicators of long-term reed development**

243   The Copernicus Sentinel satellite constellation (including, among other sensors, Sentinel-1 SAR and

244   Sentinel-2 MSI) was used as primary data source to examine how vegetation development could be

245   observed remotely. All preprocessing was done with the SNAP toolbox (v5.0) provided by the European

246   Space Agency. Sentinel-1 SAR multi-look, dual polarized (VV and VH) level-1 Ground Range Detected (GRD)

247   interferometric wide swath (IW) images were used, these data are already multi-looked. We preprocessed

248   these images by first removing thermal noise, followed by the application of an orbit file. Then data were

249   calibrated to sigma nought, and a range Doppler terrain correction was applied. We did not apply speckle

250   reduction filters as this would have decreased the spatial resolution, increasing the probability of including

251   mixed pixels (with land and water). As we are in a very flat area, at sea level we did not require additional

252   terrain corrections, hence a digital elevation model (DEM) based correction was not applied. Sentinel-2

253   MSI images, with 10m resolution, were atmospherically corrected to Bottom Of Atmosphere using a dark

254   pixel approach with the Sen2Cor tool set in SNAP. The ozone content were auto determined from the

255   auxiliary information, the aerosol determination was set to 'rural, maritime', and cirrus correction was

256   turned off. We used Sentinel images of winter, spring and summer. The seasonal timing of these images

257   matched the in situ measurements, see table 2. We focused on the RGB and NIR bands of the Sentinel

258   images, as these are required to calculate the desired vegetation indices, but also because including other

259   Sentinel 2 bands, such as vegetation red edge (bands 5-7), would have decreased our pixel size (to 20 m).

260   This would have increased the chance of including mixed pixels. A single cloud and cloud shadow was

261   removed from the Sentinel-2 images of 2016-06-07; the cloud stretched over approximately 700 meters

262   of coast. Where the cloud partially or completely covered the reed bed, the entire reed bed perpendicular

263   to the water was removed from the analysis. The average VV backscatter and VH backscatter from

264   Sentinel-1 SAR and average NDVI from Sentinel-2 MSI were compared between increasing, stable and

265   decreasing reed beds.

266

267   Table 2, Dates of in situ sampling and corresponding Sentinel-1 SAR (S1) and Sentinel-2 MSI (S2) images

268   of the Razelm Sinoe area.

In situ date	Location	Season	S1 date	S2 date
2015-3	Jurilovca	Winter	2015-01-12	2016-01-09
2015-5	Jurilovca	Spring	2015-05-12	2016-05-22
2015-7	Jurilovca	Summer	2015-07-23	2016-06-07
2016-3	Histria	Winter	2015-01-12	2016-01-09
2016-5	Histria	Spring	2015-05-12	2016-05-22
2016-7	Histria	Summer	2015-07-23	2016-06-07

269

270

271   To analyze seasonal effects, the water line was individually established for each Sentinel-2 MSI image, for

272   the first 2 images (2016-01-09 and 2016-04-28) a NDVI threshold of 0 was used (NDVI<0 was assigned

273   water). This threshold performed poorly in the July image, where water had a positive NDVI value, possibly

274   due to phytoplankton. For this image a threshold of 0.3 was used (NDVI<0.3 was assumed water). The

275   difference in NDVI between vegetated and unvegetated foreshore is typically distinct, the established

276   thresholds were checked visually and found to perform well. To exclude potential mixed pixels, we only

277   used pixels found to be vegetation in all Sentinel-2 images.

278   In addition to the NDVI, the Soil Adjusted Vegetation Index (SAVI), with a default L value of 0.5, was also

279   used as this was found to perform better than NDVI when analyzing reed vegetation (Poulin et al. 2010).

280

281   The NDVI, VV and VH backscatter of Sentinel images were compared between reeds established to be

282   declining, stable or expanding (as retrieved from the Landsat imagery). This was done for the Sentinel-1

283   SAR and Sentinel-2 MSI images of winter, spring and summer, respectively.

284

285   To establish which biophysical properties had a large effect on remote sensing imagery, we compared in

286   situ biophysical measurements with seasonally matching remote sensing images. In situ measurements

287   of biomass, vegetation height, stem diameter and stem density were compared with VV, VH backscatter

288   and NDVI at that location (the values of the corresponding pixel was extracted) using separate linear

289   regressions. The three different seasons were tested separately. Locations of the in situ stations are

290   provided in Appendix 1.

291

292

293   **Results**

294

295   **Long-term reed development from remote sensing**

296   From the Landsat optical data of 1995 and 2017, we found a vegetation loss of 38 ha (426 pixels), whereas

297   the vegetation was found to be stable in 265 ha (2944 pixels) and increased (expanded) in 1946 ha (21627

298   pixels) in a period of 22 years. The multi-year analysis showed a strong linear increase in locations labelled

299   as expanding reed (see figure 3). There was an overall decrease in reeds in locations marked as such; the

300   rate of decrease was especially large in the period 2008-2011. The water distance of stable areas also

301   increased, likely because points where the water distance was larger than 45m were also labelled as
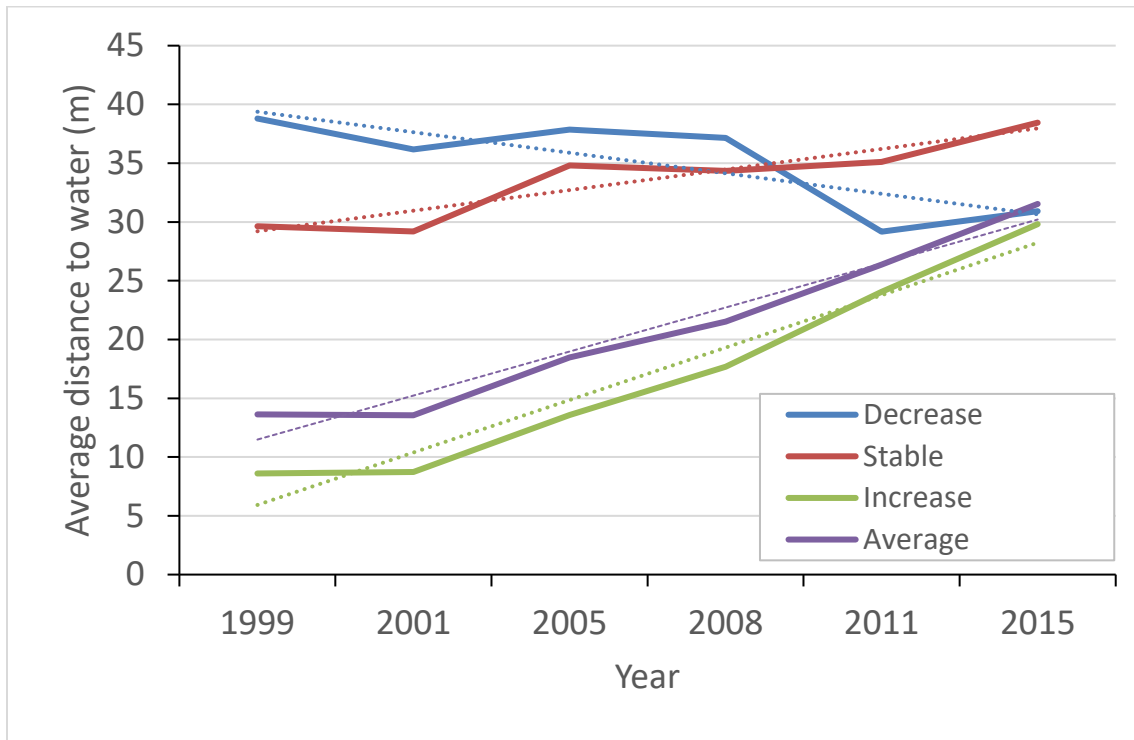
302   stable.

303

304

305   Figure 3, The multi-year development of locations with decreasing, stable and increasing reed vegetation.

306   This figure shows the development of the average distance to the water (shoreline) of the different

307   development classes (decrease n=631, stable n=4064 and increase n=16108) based on Landsat images.

308   The development class was determined over the entire period (comparing 1995 and 2017).

309

310

311

Seasonal remote sensing as indicators of long-term reed development

The Sentinel-2 optical data showed that the NDVI was lowest in winter, increases in spring and was highest in summer. Although the NDVI seemed higher in stable and increasing sites in summer, the differences between decreasing, stable and increasing reeds were small (figure 4). SAVI showed the same pattern as NDVI, with clear differences between seasons, and small differences between eroding, stable and expanding reed sites. Decreasing, stable and increasing sites could not be distinguished using optical satellite data (NDVI or SAVI).
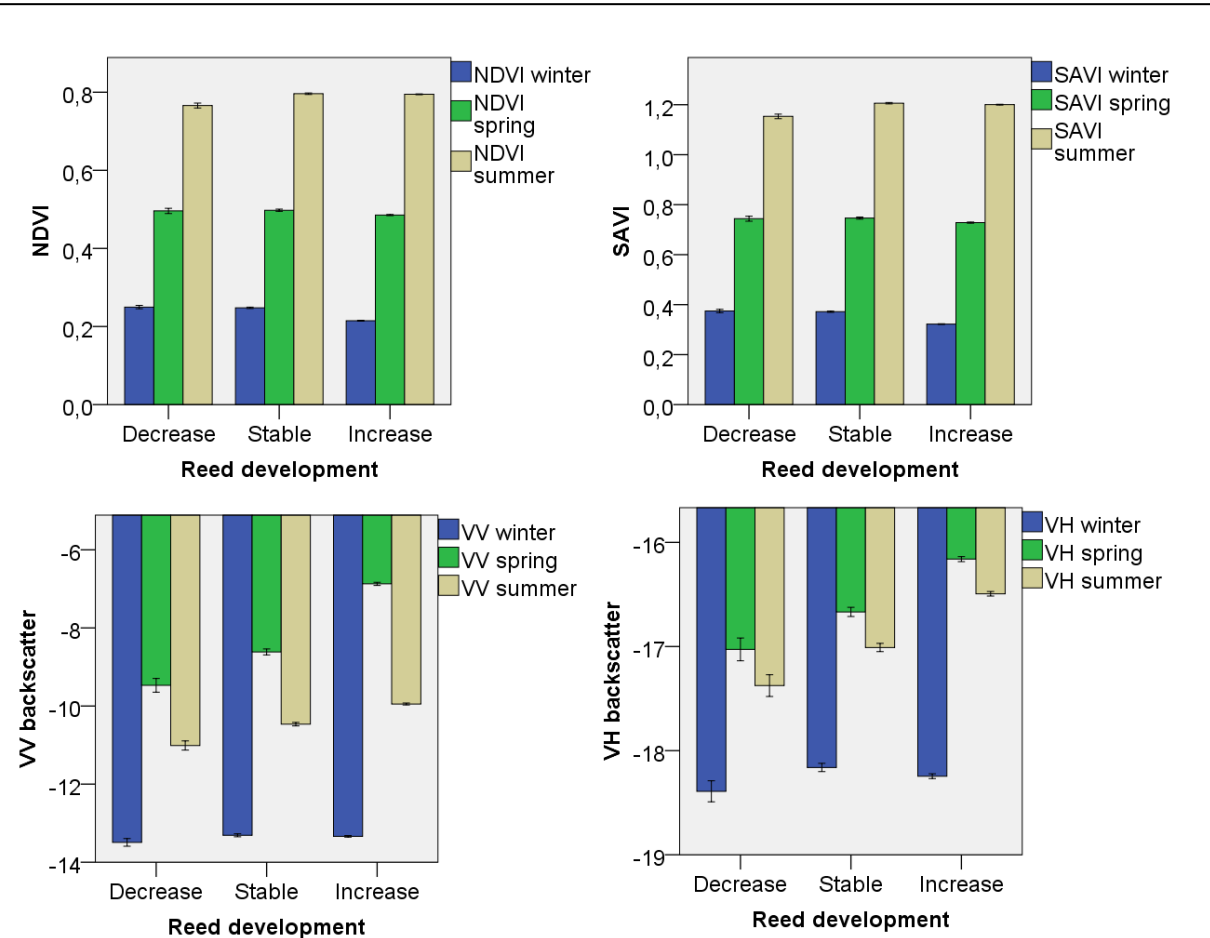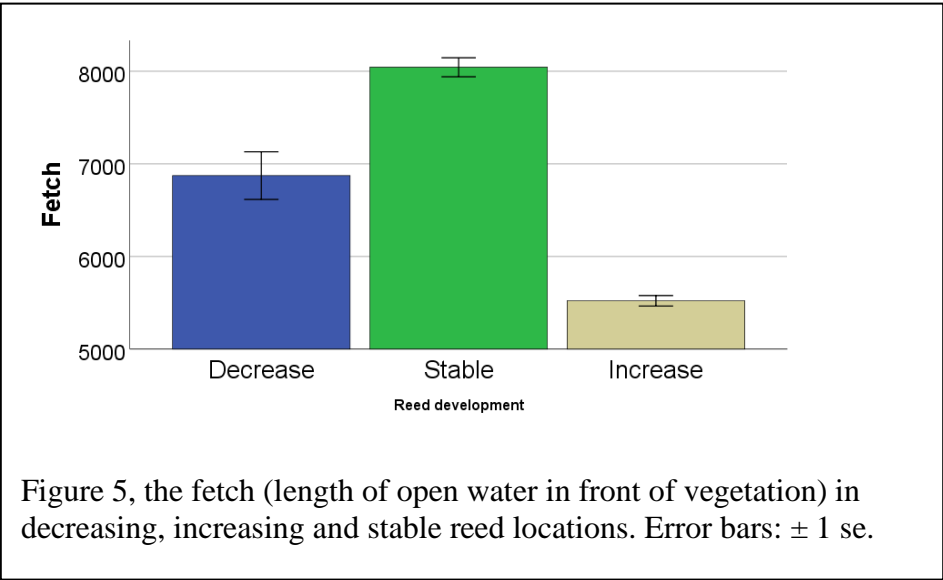

Figure 4, Seasonal patterns in optical and radar signals of decreasing, increasing and stable reed sites, in the entire Razelm Sinoe Lagoon System. Error bars: ± 1 se.

336   The Sentinel-1 SAR data showed low values for the backscatter, and hence likely "smooth vegetation"

337   (canopy largely of the same height) in winter, relatively high backscatter, and hence "rough vegetation"

338   (canopy variable in height) in spring and an intermediate backscatter and roughness in summer.

339   Interestingly, in sites with decreasing reed beds, the backscatter was low (suggesting smooth vegetation),

340   while in stable reed beds the backscatter was intermediate, and in increasing reed beds the backscatter

341   was highest (suggesting the roughest vegetation structure). This pattern (i.e., a strong contrast in

342   backscatter between the different reed development categories) was especially clear in spring, but was

343   also visible in summer. The winter backscatter was similar between decreasing, stable and increasing sites,

344   but in spring large differences had developed (see figure 4). VV and VH polarized radar showed a similar

345   pattern, the largest seasonal changes were found in the expanding reed beds, whereas the decreasing

346   reed beds showed least seasonal changes.

347   Established vegetation appeared to be able to persist in areas with a long fetch, but an increase (reed

348   expansion) mainly occurred in relatively sheltered locations (see figure 5). Areas which had a decrease in

349   reed beds, had on average an intermediate fetch but with a large spread, suggesting that die-back of reed

350   can occur regardless of fetch length. These decreasing sites also showed limited seasonal expansion, but

351   with large variation. Increasing and stable sites showed a larger seasonal expansion (see figure 6).

352

Figure 5, the fetch (length of open water in front of vegetation) in decreasing, increasing and stable reed locations. Error bars: ± 1 se.

353

354

Figure 6, the seasonal expansion of decreasing, increasing and stable locations. Error bars: ± 1 se.
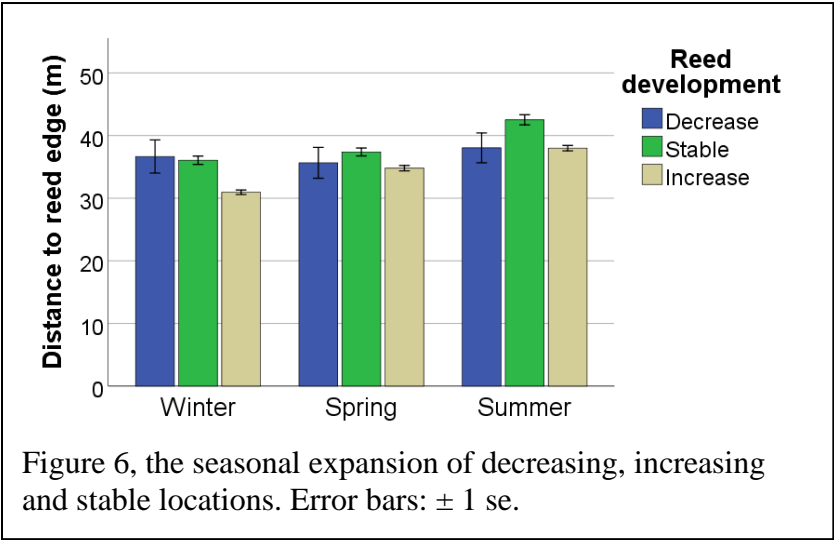
355

356

357 **Seasonal variation in properties of reed vegetation measured in situ**

358 The in situ data of both field sites show a slow reed development in spring. Biomass seemed lowest in

359 spring, possibly indicating that the vegetation had only just started to develop. However, biomass was not

18

360　significantly different between seasons. The stem diameter was highest in spring. This might be due to a

361　quicker disappearance of smaller stems. However this was not indicated by the stem density, which was

362　not significantly different between seasons. Only vegetation height was significantly higher in winter,

363　indicating that dead stems were still present in winter. All vegetation properties measured in situ showed

364　great variation (see figure 7).

365

366

367
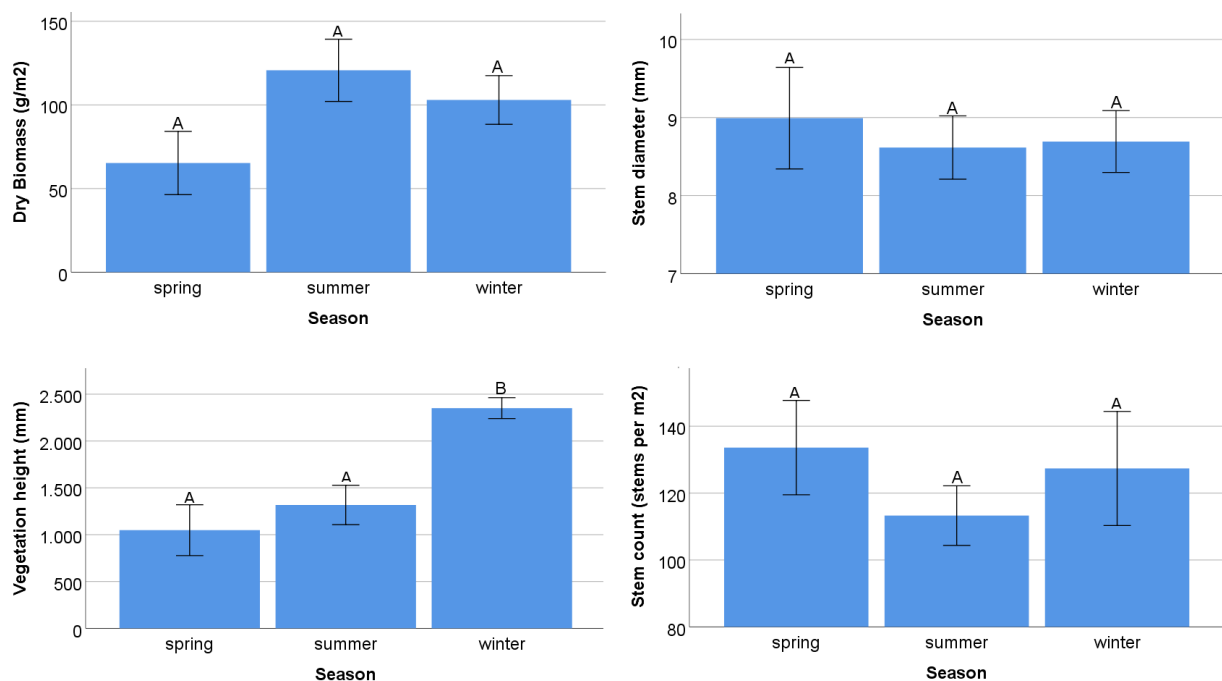
368　Figure 7. Seasonal differences between in situ measured properties of reed vegetation.

369

370

371　**Relating seasonal remote sensing indicators to in situ patterns**

372　We compared the in situ measurements with radar backscatter to explain which vegetation properties

373　cause patterns in backscatter, and hence which underlying processes can explain the seasonal differences

374　in backscatter. However, the in situ measurements showed no clear relation with backscatter.

375 We tested 36 hypotheses simultaneously, hence according to the Bonferroni correction our p-value

376 should be <0.0014 to be statistically significant, none of the tested variables met this threshold (see table

377 3 and figure 7). The in situ data did not show a strong effect on backscatter. We can therefore not

378 definitively conclude what property or process underlies the seasonal changes in backscatter.

379

380 Table 3, the seasonal relation (with linear regression statistics n, F, P and R2adj) between in situ

381 measurements of the biophysical properties of reed vegetation and remote sensing signals (NDVI, and VV

382 and VH backscatter).

			NDVI			VV			VH		
Season	Biophysical properties	n	F	P	R2adj	F	P	R2adj	F	P	R2adj
Spring	Biomass	9	1.547	0.254	0.064	0.010	0.925	-0.141	1.471	0.265	0.056
Spring	Density	14	0.564	0.467	-0.035	0.120	0.735	-0.073	1.494	0.245	0.037
Spring	Diameter	15	2.146	0.167	0.076	2.973	0.108	0.124	0.769	0.396	-0.017
Spring	Height	9	2.613	0.150	0.168	0.021	0.889	-0.139	0.013	0.914	-0.141
Summer	Biomass	15	1.468	0.247	0.032	0.003	0.960	-0.077	0.182	0.677	-0.062
Summer	Density	30	0.021	0.887	-0.035	1.309	0.262	0.011	0.336	0.567	-0.023
Summer	Diameter	37	0.067	0.797	-0.027	0.349	0.558	-0.018	0.151	0.700	-0.024
Summer	Height	15	0.865	0.369	-0.010	0.384	0.546	-0.046	2.455	0.141	0.094
Winter	Biomass	17	1.156	0.299	0.010	1.740	0.207	0.044	0.184	0.674	-0.057
Winter	Density	23	0.003	0.955	-0.047	0.491	0.491	-0.022	1.544	0.227	0.022
Winter	Diameter	29	0.025	0.877	-0.036	2.175	0.152	0.040	0.109	0.744	-0.033
Winter	Height	18	0.436	0.518	-0.034	0.192	0.667	-0.050	0.046	0.836	-0.119

383

Discussion

The aim of this study was to 1) establish an indicator to enable monitoring of reed-wetland dynamics and thereby the ecosystem service stability, and 2) apply it to the Razelm Sinoe Lagoon System in Romania to establish the stability of these reed wetlands. We used optical and radar satellite data to compare increasing, decreasing and stable reed edges of wetlands and found that especially the seasonal differences in radar backscatter provides valuable insight into the long-term vegetation stability. That is, indicators based on optical data showed no difference between the areas, but indicators based on SAR data showed large differences between decreasing, stable and increasing reed lands. All sites are roughest in spring, smoother in summer and smoothest in winter. In general, the expanding sites are roughest, the decreasing sites are smoothest. In addition, the differences between winter, spring and summer are largest in expanding sites, intermediate in stable sites and smallest in decreasing sites.

When analyzing vegetation stress near the waters edge using remote sensing, mixed pixels that contain both land and water potentially affect the results. We tried to reduce their influence as much as possible by selecting only pixels that are classified as land in all images. Any remaining mixed pixels in the analysis are expected to affect all classes equally and therefore would not cause the differences between classes. It could be argued that decreasing sites have decreased further and will therefore contain more mixed pixels. However, we established increasing and decreasing states of reed development based on a 2017 image, and calculated the backscatter on earlier images (2015 and 2016). Therefore, continued development cannot have increased the number of mixed pixels. Finally, if mixed pixels significantly affected our results, this would have been detected by our optical indicators (NDVI, SAVI), which are known to be sensitive towards vegetative vs non-vegetative states. These indicators showed no differences between increasing and decreasing areas. It is therefore unlikely that the detected difference is due to the effect of mixed pixels.

Seasonal remote sensing as indicators of long-term reed development

We expect that the magnitude of the observed patterns in seasonal development of roughness to be site specific, due to climatological differences and site-specific differences in local environmental conditions. However, the seasonal pattern of a slower development and smaller seasonal differences in retreating sites is expected to be more general. A decrease in development and recovery speed after disturbance at vulnerable sites is also described by the critical slowing down theory (Scheffer et al. 2001). This theory indicates that as resilience decreases, the system takes longer to recover from disturbance. This could explain the limited and lower seasonal expansion at decreasing sites, which would have a lower resilience. However, although the first experimental evidence of this theory in wetlands is starting to emerge (van Belzen et al. 2017), the application of this theory to reed-lands has yet to be tested. This theory also indicates that plants can remain seemingly healthy up to a collapse, and that optical measurements related to biomass (such as NDVI) are ineffective for measuring resilience. In our study, we also found little response to lateral change in the reed beds in the optical data. However it is unclear if the observed differences in radar backscatter are related to a decrease in resilience or caused by another biophysical process. Notably, the large seasonal variation in backscatter at the expanding site should not be misinterpreted as flickering, which is often regarded as an indicator of nearness of collapse (Dakos et al. 2013). The seasonal variation seems to rather indicate growth vigor.

A multi-seasonal approach is known to be important when studying reed vegetation (Poulin et al. 2010, Lee et al. 2012). Hence seasonal changes were expected to hold information on potential lateral increase or decrease of the reed. There was a clear seasonal trend in the lateral extent of the reed bed, with reed beds protruding into the lake in summer. However the seasonal difference in backscatter in the reed bed vegetation between decreasing stable and increasing reed beds has not been described before. The early growing season is known to be very important for reed, as reed particularly depends on its initial growth

432   to establish competitive dominance (Yamasaki and Tange 1981). The differences in backscatter between

433   decreasing, stable and increasing sites could therefore be due to an earlier start of growth at more

434   favorable locations. However, this would likely also create a difference in biomass, which would have been

435   detectable by optical satellites. A previous study also found little use for NDVI in reed vegetation, but SAVI

436   performed well (Poulin et al. 2010). However, in our study SAVI performed very similar to NDVI; neither

437   of them showed a difference in reed vegetation between expanding, retracting and stable sites.

438

439   Radar data is able to provide valuable information on roughness that we could not derive from optical

440   remote sensing. However it remains unclear what the underlying processes are. Graham and Harris

441   (Graham and Harris 2003) created a water cloud model to simulate radar backscatter. They identified the

442   most important factors in radar backscatter as the thickness of the vegetation layer (the vegetation

443   height), the internal properties of the vegetation layer (leaf area index or leaf properties), the vegetation

444   moisture content and the soil moisture content. We expect that if the seasonal differences in backscatter

445   between increasing and decreasing locations were caused by thickness or the properties of the vegetation

446   layer we would have detected it in the NDVI. Although indices such as NDVI are known to become

447   insensitive at higher values (Baret and Guyot 1991, Zhang et al. 2013), the NDVI did show seasonal

448   differences, indicating it was not saturated in all seasons. However, we cannot rule out properties of the

449   vegetation layer, such as internal leaf structure, that do not affect NDVI but could have affected radar

450   backscatter.

451

452   Vegetation and soil moisture content are major contributors in the water cloud model. The water cloud

453   model is often used to simulate radar backscatter of land based vegetation (Graham and Harris 2003). The

454   additional water layer in case of flooded vegetation is expected to have an even larger effect on

455   backscatter than soil moisture content, even though the reed vegetation above it is over 2m. This water

456   layer is likely largely affected by elevation, as reed at lower elevations has to highest chance of being

457   flooded. Retraction and expansion of the reed may also be a function of elevation. However, a large

458   difference in suitability of conditions for reed growth would likely also have been visible in the optical

459   data. Further study, likely combining remote sensing with an extensive field measurement campaign, will

460   be required to establish which biophysical or environmental factors causes the seasonal difference

461   between radar backscatter of decreasing, stable and increasing reed beds.

462

463

464   **Long-term reed development from remote sensing**

465   Our analysis showed that in the Razelm Sinoe Lagoon System reed is, overall, expanding. We found an

466   average expansion of 87 ha per year between 1995 and 2017, clearly showing that the massive reed die-

467   back found elsewhere in Europe does not extend to the Danube - Black Sea System. Although reed die-

468   back has been found in southern Europe (Fogli et al. 2002, Cerri et al. 2017) our findings support earlier

469   notions that reed is expanding (Van Der Putten 1997). The reed expansion although large in surface area

470   is still relatively small when compared with the area of the entire lagoon system. On average the

471   expansion is about 1.1 meter per year. A study in the United States, where reed is considered to expand

472   rapidly and management is focused on removing reed, found an invasion rate between 0.1-0.7 meter per

473   year, depending on which species it was competing with (Silliman and Bertness 2004). It is important to

474   note that these are invasion and not expansion rates. In this light the expansion rate found in Romania

475   can be considered rapid. However, it should be kept in mind that this long-term analysis was done using

476   the Landsat satellites; the relatively low resolution of this satellite makes precise estimates difficult. Yet,

477   our Landsat time-series demonstrated that the trends are persistent, with the strongest decrease in the

478   period 2008-2011.

479

480   Given the large reed area that is persistently present, it is clear that the ecosystem services are clearly not

481   threatened by reed die-back. However, a too strong reed expansion might still be a risk for service

482   stability. Anthropogenic influences have increased influence of the Danube river and limited exchange

483   with the Black Sea during the past century (Hanganu et al. 1999, 2002, Stanica et al. 2012). As a result the

484   lagoon system has become mainly a fresh water system and is collecting organic and non-organic matter

485   (Stanica et al. 2012), with the Sinoe Lagoon the only notable exception, as it has turned towards natural

486   evolution and a trend towards brackish waters since mid 2000s, when the previously controlled

487   engineered inlets were left in natural flow. Reed is known for its capability to absorb nutrients such as

488   nitrogen from water (Findlay et al. 2002), because of this ability it is often applied in helophyte filters. This

489   means it will clean water passing through the lagoon, but also trap many nutrients there.

490   If the system continues to accumulate sediments and the elevation increases to the point where it offers

491   suitable growing conditions to reed throughout the lagoon, a sudden explosive reed expansion could

492   threaten open water dependent ecosystem services and the corresponding economic benefits. To ensure

493   long term service stability, this situation will have to be monitored carefully.

494

495   Our analyses showed that reed expansion mainly occurred in sheltered areas, whereas exposed areas

496   were mainly stable or decreasing. An increased establishment at sheltered sites was also indicated by

497   Coops et al. (1994) in the Netherlands. In contrast, Weisner (1987) found a rapid expansion of reed at

498   exposed sites in Sweden. However, Weisner (1987) pointed out that an elevation difference likely created

499   by a different grazing regime might be the underlying cause for the rapid expansion. In general, Weisner

500   (1987) too expected a more rapid expansion at sheltered sites. This may be associated with wave forcing,

501   which is known to have a large influence on reed development (Haslam 1970, Coops et al. 1991), and has

502   been shown to effect seedling establishments in other marsh species (Cao et al. 2019).

503

504

Conclusions and outlook

505 **Conclusions and outlook**

506 We developed an indicator that can help predict the stability of reed wetlands, based on the size of

507 seasonal differences in radar backscatter. We found that decreasing areas had smaller seasonal changes

508 than stable or increasing areas. Radar backscatter signals showed differences among expanding, stable

509 and retracting reed beds, where optical data did not. Although further study to pinpoint the biophysical

510 processes underlying the radar signal would be recommended, its application has already proven to be

511 very useful. It would also be interesting to incorporate a higher temporal resolution, i.e. analyse multiple

512 images per season to better assess variations within and among seasons. We expect that our technique

513 can easily be adapted to similar ecosystems such as salt marshes, but can also be applied to terrestrial

514 systems such as heathlands or grasslands. In heathlands, SAR is also known to contribute new information

515 not obtainable through optical data alone (Schmidt et al. 2018) and heathlands are known to adjust their

516 seasonal development based on local conditions (Specht et al. 1983). This technique might even be

517 applied to forests, where SAR is already often used to establish biomass (Luckman et al. 1998), but

518 seasonal variation has not yet been used to assess the service stability. However, the great difficulties

519 associated with mapping foliage dynamics in forests using SAR (Proisy et al. 2000), suggests that the radar

520 backscatter indicator identified in the current study is likely best suited to characterize highly dynamic

521 systems, which produce large seasonal differences.

522

523

Declarations

Conflicts of interest/Competing interests: Not applicable

Ethics approval: Not applicable

Consent to participate: Not applicable

Consent for publication: Not applicable

Availability of data and material: Fully available through: https://easy.dans.knaw.nl/ui/home

Code availability: Fully available through: https://easy.dans.knaw.nl/ui/home

Author contributions

BO and DvdW planned the research. ASC, supported by local staff, collected the field data. BO and ASC

processed and analyzed the data. BO and DvdW wrote the paper. BO, ASC, TJB, AST and DvdW refined the

paper. All authors read and approved the final manuscript.

Acknowledgements

Methods and Ethics Approval

All field activities were performed as part of the annual access and permits GeoEcoMar has received from

the Danube Delta Biosphere Reserve Administration. Each field survey was announced and access was

requested to the Biosphere Reserve Administration, as stated in the permits received. All results of all

549   GeoEcoMar studies are delivered anually to the Danube Delta Biosphere Reserve Administration and they

550   are part of the scientific basis that drives the integrated management of the Danube Delta territory.

551

552   **References**

553   Baghdadi, N., M. Bernier, R. Gauthier, and I. Neeson. 2001. Evaluation of C-band SAR data for wetlands

554   mapping. International Journal of Remote Sensing 22:71–88.

555   Barbier, E. B., E. W. Koch, B. R. Silliman, S. D. Hacker, E. Wolanski, J. Primavera, E. F. Granek, S. Polasky,

556   S. Aswani, and L. A. Cramer. 2008. Coastal ecosystem-based management with nonlinear ecological

557   functions and values. science 319:321–323.

558   Baret, F., and G. Guyot. 1991. Potentials and limits of vegetation indices for LAI and APAR assessment.

559   Remote sensing of environment 35:161–173.

560   van Belzen, J., J. van de Koppel, M. L. Kirwan, D. van der Wal, P. M. J. Herman, V. Dakos, S. Kéfi, M.

561   Scheffer, G. R. Guntenspergen, and T. J. Bouma. 2017. Vegetation recovery in tidal marshes reveals

562   critical slowing down under increased inundation. Nature Communications 8:ncomms15811.

563   Boesch, D. F., and R. E. Turner. 1984. Dependence of fishery species on salt marshes: the role of food

564   and refuge. Estuaries 7:460–468.

565   Bourgeau-Chavez, L. L., K. P. Kowalski, M. L. C. Mazur, K. A. Scarbrough, R. B. Powell, C. N. Brooks, B.

566   Huberty, L. K. Jenkins, E. C. Banda, and D. M. Galbraith. 2013. Mapping invasive Phragmites

567   australis in the coastal Great Lakes with ALOS PALSAR satellite imagery for decision support.

568   Journal of Great Lakes Research 39:65–77.

569   Brisco, B., M. Kapfer, T. Hirose, B. Tedford, and J. Liu. 2011. Evaluation of C-band polarization diversity

570   and polarimetry for wetland mapping. Canadian Journal of Remote Sensing 37:82–92.

571   Brix, H. 1999. The European research project on reed die-back and progression (EUREED). Limnologica-

572   Ecology and Management of Inland Waters 29:5–10.

573   Cao, H., Z. Zhu, R. James, P. M. J. Herman, L. Zhang, L. Yuan, and T. J. Bouma. 2019. Wave effects on

574   seedling establishment of three pioneer marsh species: survival, morphology and biomechanics.

575   Annals of botany.

576   Cerri, M., R. Sapkota, A. Coppi, V. Ferri, B. Foggi, D. Gigante, L. Lastrucci, R. Selvaggi, R. Venanzoni, M.

577   Nicolaisen, F. Ferranti, and L. Reale. 2017. Oomycete Communities Associated with Reed Die-Back

578   Syndrome. Frontiers in Plant Science 8:1–11.

579   Chambers, R. M., L. a. Meyerson, and K. Saltonstall. 1999. Expansion of *Phragmites australis* into tidal

580   wetlands of North America. Aquatic Botany 64:261–273.

581   Chmura, G. L. 2011. What do we need to assess the sustainability of the tidal salt marsh carbon sink?

582   Ocean & Coastal Management 83: 25-31.

583   Coops, H., R. Boeters, and H. Smit. 1991. Direct and indirect effects of wave attack on helophytes.

584   Aquatic Botany 41:333–352.

585   Coops, H., N. Geilen, and G. van der Velde. 1994. Distribution and growth of the helophyte species

586   Phragmites australis and Scirpus lacustris in water depth gradients in relation to wave exposure.

587   Aquatic Botany 48:273–284.

588   Dakos, V., E. H. van Nes, and M. Scheffer. 2013. Flickering as an early warning signal. Theoretical ecology

589   6:309–317.

590   Deegan, L. A., J. E. Hughes, and R. A. Rountree. 2002. Salt marsh ecosystem support of marine transient

591   species. Pages 333–365. Concepts and controversies in tidal marsh ecology. Springer.

592   Dinu, I., G. Umgiesser, M. Bajo, F. de Pascalis, A. Stănică, C. Pop, R. Dimitriu, I. Nichersu, and A.

593   Constantinescu. 2015. Modelling of the response of the Razelm-Sinoe Lagoon system to physical

594   forcing. GeoEcoMarina. doi: https://doi.org/10.5281/zenodo.45064.

595   Findlay, S. E. G., S. Dye, and K. A. Kuehn. 2002. Microbial growth and nitrogen retention in litter of

596   Phragmites australis compared to Typha angustifolia. Wetlands 22:616–625.

597   Fogli, S., R. Marchesini, and R. Gerdol. 2002. Reed (Phragmites australis) decline in a brackish wetland in

598   Italy. Marine Environmental Research 53:465–479.

599   Freeman, A., and S. L. Durden. 1998. A three-component scattering model for polarimetric SAR data.

600   IEEE Transactions on Geoscience and Remote Sensing 36:963–973.

601   Graham, a. J., and R. Harris. 2003. Extracting biophysical parameters from remotely sensed radar data: a

602   review of the water cloud model. Progress in Physical Geography 27:217–229.

603   de Groot, A. V, R. M. Veeneklaas, D. P. J. Kuijper, and J. P. Bakker. 2011. Spatial patterns in accretion on

604   barrier-island salt marshes. Geomorphology 134:280–296.

605   Guo, L., D. W. Ott, and T. J. Cutright. 2014. Accumulation and histological location of heavy metals in

606   Phragmites australis grown in acid mine drainage contaminated soil with or without citric acid.

607   Environmental and Experimental Botany 105:46–54.

608   Hanganu, J., D. Dubyna, E. Zhmud, I. Grigoras, U. Menke, H. Drost, N. Ştefan, and I. Sărbu. 2002.

609   Vegetation of the Biosphere Reserve "Danube Delta." RIZA report 2002.049.

610   Hanganu, J., G. Mihail, and H. Coops. 1999. Responses of ecotypes of Phragmites australis to increased

611   seawater influence: a field study in the Danube Delta, Romania. Aquatic Botany 64:351–358.

612   Haslam, S. M. 1970. The performance of Phragmites communis Trin. in relation to water-supply. Annals

613   of Botany 34:867–877.

614   Henderson, F. M., and A. J. Lewis. 2008. Radar detection of wetland ecosystems: a review. International

615   Journal of Remote Sensing 29:5809–5835.

616   Koch, E. W., E. B. Barbier, B. R. Silliman, D. J. Reed, G. M. E. Perillo, S. D. Hacker, E. F. Granek, J. H.

617   Primavera, N. Muthiga, and S. Polasky. 2009. Non-linearity in ecosystem services: temporal and

618   spatial variability in coastal protection. Frontiers in Ecology and the Environment 7:29–37.

619   Lee, Y.-K., J.-W. Park, J.-K. Choi, Y. Oh, and J.-S. Won. 2012. Potential uses of TerraSAR-X for mapping

620   herbaceous halophytes over salt marsh and tidal flats. Estuarine, Coastal and Shelf Science

621   115:366–376.

622   Luckman, A., J. Baker, M. Honzák, and R. Lucas. 1998. Tropical forest biomass density estimation using

623   JERS-1 SAR: Seasonal variation, confidence limits, and application to image mosaics. Remote

624   Sensing of Environment 63:126–139.

625   Möller, I. 2006. Quantifying saltmarsh vegetation and its effect on wave height dissipation: Results from

626   a UK East coast saltmarsh. Estuarine, Coastal and Shelf Science 69:337–351.

627   Morgan, P. A., D. M. Burdick, and F. T. Short. 2009. The functions and values of fringing salt marshes in

628   northern New England, USA. Estuaries and Coasts 32:483–495.

629   Ostendorp, W., M. Dienst, and K. Schmieder. 2003. Disturbance and rehabilitation of lakeside

630   Phragmites reeds following an extreme flood in Lake Constance (Germany). Hydrobiologia 506–

631   509:687–695.

632   Pengra, B. W., C. A. Johnston, and T. R. Loveland. 2007. Mapping an invasive plant, Phragmites australis,

633   in coastal wetlands using the EO-1 Hyperion hyperspectral sensor. Remote Sensing of Environment

634   108:74–81.

635   Poulin, B., A. Davranche, and G. Lefebvre. 2010. Ecological assessment of Phragmites australis wetlands

636   using multi-season SPOT-5 scenes. Remote Sensing of Environment 114:1602–1609.

637   Proisy, C., E. Mougin, E. Dufrêne, and V. Le Dantec. 2000. Monitoring seasonal changes of a mixed

638   temperate forest using ERS SAR observations. IEEE Transactions on Geoscience and Remote

639   Sensing 38:540–552.

640   Van Der Putten, W. H. 1997. Die-back of Phragmites australis in European wetlands: An overview of the

641   European Research Programme on Reed Die-back and Progression (1993-1994). Aquatic Botany

642   59:263–275.

643   Reschke, J., A. Bartsch, S. Schlaffer, and D. Schepaschenko. 2012. Capability of C-band SAR for

644   operational wetland monitoring at high latitudes. Remote Sensing 4:2923–2943.

645   Scheffer, M., S. Carpenter, J. A. Foley, C. Folke, and B. Walker. 2001. Catastrophic shifts in ecosystems.

646   Nature 413:591–596.

647   Schmidt, J., F. E. Fassnacht, M. Förster, and S. Schmidtlein. 2018. Synergetic use of Sentinel-1 and

648   Sentinel-2 for assessments of heathland conservation status. Remote Sensing in Ecology and

649   Conservation 4:225–239.

650   Silliman, B. R., and M. D. Bertness. 2004. Shoreline Development Drives Invasion of Pragmites australis

651   and the Loss of Plant Diversity on New England Salt Marshes. Conservation Biology 18:1424–1434.

652   Specht, R. L., E. J. Moll, F. Pressinger, and J. Sommerville. 1983. Moisture regime and nutrient control of

653   seasonal growth in Mediterranean ecosystems. Pages 120–132Mediterranean-type ecosystems.

654   Springer.

655   Stanica, A., J. Bujini, and D. Stefanescu. 2012. ARCH RAPORT RAZELM SINOE[EN].

656   Volesky, L. A., S. Iqbal, J. J. Kelly, and P. Geddes. 2018. Relationships of Native and Exotic Strains of

657   Phragmites australis to Wetland Ecosystem Properties. Wetlands 38:577–589.

658   Weisner, S. E. B. 1987. The relation between wave exposure and distribution of emergent vegetation in

659   a eutrophic lake. Freshwater Biology 18:537–544.

660   Yamasaki, S., and I. Tange. 1981. Growth responses of Zizania latifolia, Phragmites australis and

661   Miscanthus sacchariflorus to varying inundation. Aquatic Botany 10:229–239.
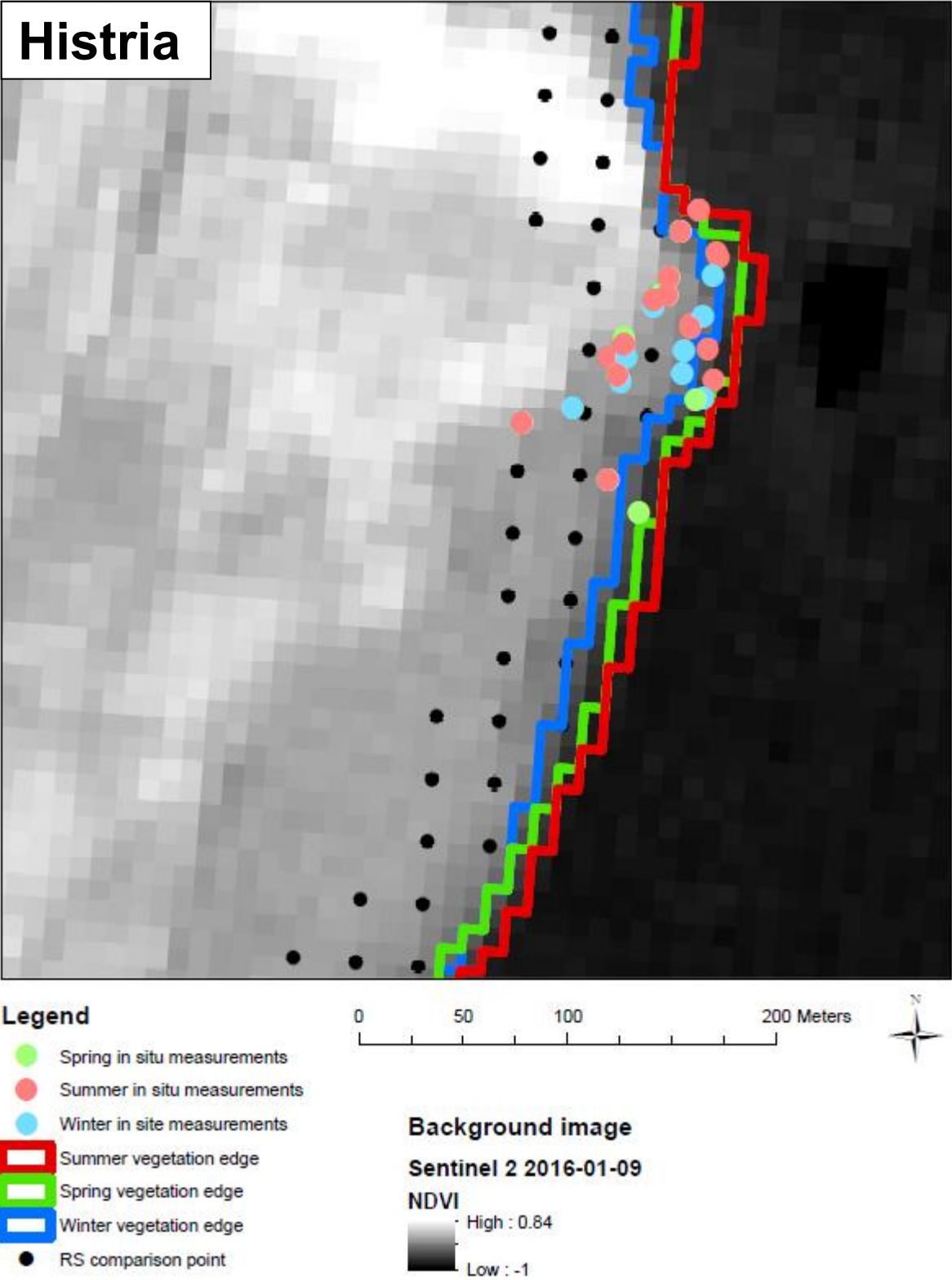
662   Zhang, Q., C. Schaaf, and K. C. Seto. 2013. The vegetation adjusted NTL urban index: A new approach to

663   reduce saturation and increase variation in nighttime luminosity. Remote Sensing of Environment

664   129:32–41.

665

666

667

Appendix 1, map of Romanian sample sites

Histria

Legend

- ● Spring in situ measurements
- ● Summer in situ measurements
- ● Winter in site measurements
- ▭ Summer vegetation edge
- ▭ Spring vegetation edge
- ▭ Winter vegetation edge
- ● RS comparison point

0   50   100   200 Meters

Background image

Sentinel 2 2016-01-09

NDVI
High : 0.84
Low : -1

Jurilovka

Legend

- Spring in situ measurements
- Summer in situ measurements
- Winter in site measurements
- Summer vegetation edge
- Spring vegetation edge
- Winter vegetation edge
- RS comparison point

0 50 100 200 Meters

Background image

Sentinel 2 2016-01-09

NDVI
- High : 0.64
- Low : -0.67

671   Appendix 2, cloud masks

672

Cloud masks

Legend

- Sample points
- Multi-year compounding cloud mask
- Dead vegetation mask

Kilometers
0   2.5   5   10

Source: Esri, DigitalGlobe, GeoEye, Earthstar Geographics, CNES/Airbus DS, USDA, USGS, AeroGRID, IGN, and the GIS User Community